Superoleophobic Surfaces through Control of Sprayed-on Stochastic Topography

Raymond Campos[1], Andrew J. Guenthner,[2] Adam J. Meuler, [3] Anish Tuteja,[4] Robert E. Cohen,[5] Gareth H. McKinley,[6] Timothy S. Haddad,[1] and Joseph M. Mabry[2]**

[1]ERC Incorporated, Air Force Research Laboratory
Edwards AFB, CA 93524
[2]Propulsion Directorate, Air Force Research Laboratory
Edwards AFB, CA 93524
[3]National Research Council / Air Force Research Laboratory
Edwards AFB, CA 93524
[4]Department of Materials Science and Engineering, The University of Michigan
Ann Arbor, MI 48109
[5]Department of Chemical Engineering, Massachusetts Institute of Technology
Cambridge, MA 02139
[6]Department of Mechanical Engineering, Massachusetts Institute of Technology
Cambridge, MA 02139
AUTHOR EMAIL ADDRESS andrew.guenthner@edwards.af.mil

RECEIVED DATE (to be automatically inserted after your manuscript is accepted if required according to the journal that you are submitting your paper to)

Abstract

The liquid repellence and surface topography characterstics of coatings comprising a sprayed-on mixture of fluoroalkyl-functional precipitated silica and a fluoropolymer binder were examined using contact and sliding angle analysis, electron microscopy, and image analysis for determination of fractal dimensionality. The coatings proved to be an especially useful class of liquid repellent materials due to their combination of simple and scalable deposition process, low surface energy, and the roughness characteristics of the aggregates. These characteristics interact in a unique way to prevent the build-up

Approved for public release, distribution unlimited.

of binder in interstitial regions, preserving re-entrant curvature across multiple length scales, thereby enabling a wide range of liquid repellency, including superoleophobicity. In addition, rather than accumulating in the interstices, the binder becomes widely distributed across the surface of the aggregates, enabling a mechanism in which a simple shortage or excess of binder controls the extent of coating roughness at very small length scales, thereby controlling the extent of liquid repellence

1. Introduction

A significant advance in the field of liquid repellence, the creation of surfaces exhibiting superoleophobicity has generated much interest since 2007.[1] The unusual characteristics of superoleophobic surfaces in contact with fuels, oils, and greases, including contact angles in excess of 150°, droplet sliding angles approaching zero, and robust metastability of the partially wetted (Cassie-Baxter) state,[2-5] provide exceptional liquid repellence with applications in machinery,[6] fabrics,[7,8] energy efficiency,[9] and protection from fouling and hazardous materials.[10] After only very sporadic previous reports,[11,12] researchers have recently created many types of superoleophobic surfaces, with new reports appearing at a very rapid pace.[1-4,7,8,13-27] Fabrication methods involve dip coating, electrospinning,[1,2,7,8] spray coating,[14,16] and templating. Among these, spray coating provides the advantages of great simplicity, scalability, speed, and compatibility with almost any substrate type (if post-processing is limited to drying at low temperature and appropriate solvents are selected). Thus, there remains a significant need for further development of superoleophobic surfaces formed by spray coating, as well as for simple means of tuning the liquid repellence of such surfaces.

Herein, we describe the development of a set of materials and methods for producing spray-coated surfaces with liquid repellence characteristics ranging from hydrophobic to superoleophobic (toward hydrocarbons as light as dodecane) that address the challenges of scalable, affordable fabrication and straightforward tuneability. The simple and robust process for fabricating these surfaces utilizes fluoroalkylsilane-treated precipitated silica aggregates ("FF-silica"), the synthesis of which we have previously reported.[28] The coating formulation also includes a Viton® fluoropolymer binder, and

a fluorinated solvent (AK-225G). This combination resulted in a wide range of stochastic surface topographies and very low surface energy values. (This combination of materials has also been widely utilized to achieve high levels of abrasion, wear, and scratch resistance.[29]) Roughness on multiple length scales below 10 μm, along with the propensity to form surfaces with re-entrant curvature, were observed to be key factors that enabled these surfaces to exhibit a wide range of liquid repellency. In addition, the ability to control the fine-scale texture by altering the amount of binder in the system was found to be a convenient geometric tuning mechanism for shaping the liquid repellence characteristics of these randomly textured, sprayed-on surfaces.

2. Materials and Methods

2.1 Preparation of Fluoroalkyl-Functional Silica (FF-Silica): Precipitated silica aggregates (HiSil 233, from PPG Industries) were treated with (1,1,2,2-tetrahydroperfluorodecyl)-dimethylchlorosilane using a previously described method.[28] Relevent physical properties of the modified silica aggregates can be found in Table S1 of Supporting Information. The aggregates, in the form of the as-dried powder, were stored under ambient atmosphere prior to use.

2.2 Spray-Deposition: Coatings were formulated from a stock mixture of 5 mg/mL ©Viton ETP-600S fluoropolymer (DuPont) in Asahiklin AK-225G (1,3-dichloro-1,2,2,3,3-pentafluoropropane; AGC Chemicals Americas). FF-silica was suspended into this mixture at 0-90 wt% silica/total solids using rapid agitation with a magnetic stir bar. Additional solvent was added to maintain a total solids concentration of 5 mg/mL, followed by 60 minutes of continued stirring. To prevent settling, spraying of the stirred suspension was always completed within 15 minutes of the cessation of stirring, and only freshly prepared batches of stirred suspension were utilized. The suspension was spray coated onto 1″ silicon wafers (P-type; 100-orientation, Wafer World, pre-cleaned by rinsing with acetone followed by drying via immersion in a stream of flowing nitrogen) through an airbrush (Paasche, VLSTPRO) with a 1.06 mm diameter tip using compressed air (25 psi). The airbrush was repeatedly passed over the substrate laterally at an approximate distance of 15-20 cm from the substrate until 20 mL of the coating mixture had been deposited. The resultant deposition level is around is 20 mg/cm^2. Following spray

coating, samples were air dried for 1 hr followed by drying for 12 hrs at 60 °C (ambient atmosphere) in a laboratory oven.

2.3 Contact Angle Measurements: Advancing (θ_{adv}) and receding (θ_{rec}) contact angles were measured using a VCA 2000 goniometer (AST, Inc.) as probe fluid was added or removed from ~ 5 µL sessile droplets. Sliding angles were measured with a Rame-Hart Model 590 goniometer on ~15-20 µL droplets. Measurements were made at multiple locations in each sample, with the standard deviation from all measurements being reported as the characteristic uncertainty in Table S2 of Supporting Information. For comparison, additional measurements on several samples with different surface composition/probing liquid combinations were made on a Dataphysics OCA20 goniometer equipped with a TBU90 tilting stage, and no significant differences were found.

2.4 Surface Characterization: Cross-sectioned samples were prepared by embedding coatings in epoxy and then sectioning the embedded sample using a PT-X ultramicrotome (RMC Products) using the recommended methodology specified for the instrument by Boeckeler, Inc.. Gold-sputtered cross-section and plan view (top down) samples were imaged using an FEI Quanta 600 scanning electron microscope. Cross-sections over a wide range of magnifications (generally 100 – 6000 x) were collected for quantitative analysis of the surface geometry, with a minimum of 5 images per condition being analyzed for samples with a highly uniform geometrical features, and 5 – 10 additional images analyzed for samples (particularly 40% FF-silica loading) that appeared to show some variability from location to location at higher magnification, in order to ensure that a representative sample of images was collected for analysis.

3. Results and Discussion

3.1 Liquid repellence and qualitative description of the effect of surface texture and spray coating process: The wide range of liquid repellency of the sprayed-on surfaces based on the combination of precipitated silica aggregates, fluoropolymer binder, and AK225G is illustrated in Fig. 1. At low FF-silica loading levels, the Wenzel (fully wetted) state exists for all liquids studied, with

advancing contact angles that are typical of highly fluorinated surfaces.[30,31] As the FF-silica loading level increases, however, the Cassie-Baxter state becomes prevalent, starting at approx. 20 wt% FF-silica for water and, at higher loading levels, for liquids of progressively lower surface tension. The switch from Wenzel to Cassie-Baxter state is readily indicated by the changes in receding contact and sliding angles, which, though not as abrupt as in regularly patterned surfaces, are still quite substantial.

As indicated by the more detailed liquid repellence map in Fig. 2, a generally simple, monotonic, and gradual relationship exists between the surface tension of the contacting liquid and the FF-silica loading level required for attaining the Cassie-Baxter state. Although Fig. 2 applies directly only for the specific set of spraying parameters reported herein, it should be noted that the spray process includes an annealing step above the glass transition of the polymer binder, which allows for relaxation of any residual stresses and some equilibration, even after the solvent has evaporated. As a result, we expect that the behavior illustrated in Fig. 2 would exhibit a low sensitivity to variations in processing parameters, provided that a similar overall density of solids is deposited on the surface. (Both imaging and contact angle measurements taken from multiple spray coating runs showed very good reproducibility of both surface texture and liquid repellence). The existence of the simple and robust relationship seen in Fig. 2 enables quantification of the trade-offs (often driven by the need to simultaneously satisfy multiple performance criteria) required to obtain a desired degree of liquid repellence, and suggests that even complex, randomly textured surfaces may be systematically altered in a straightforward manner by altering the ratio of aggregates to binder in order to control liquid repellence.

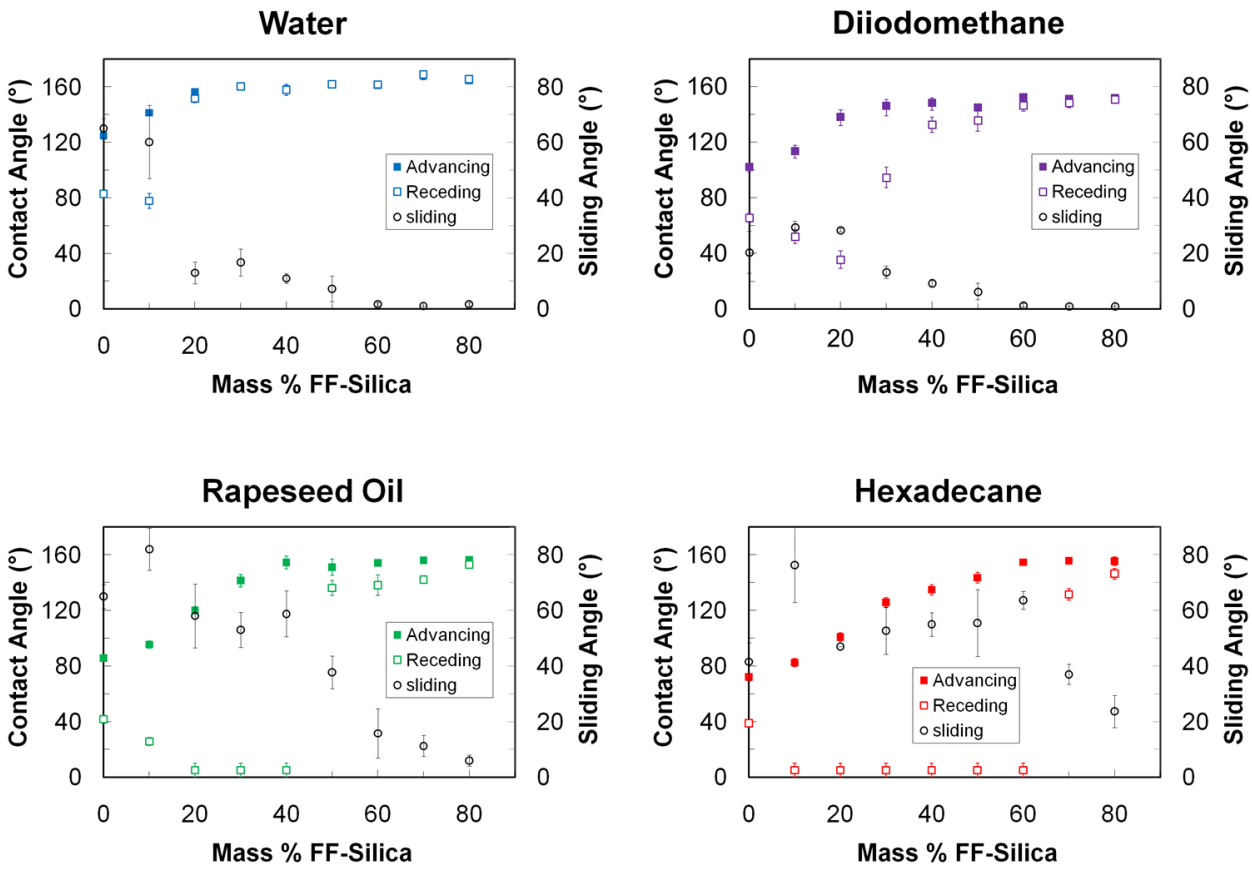

Figure 1. Apparent advancing, receding, and sliding contact angle measurements of water (γ_{lv} = 72.1 mN/m), diiodomethane (γ_{lv} = 50.8 mN/m), rapeseed oil (γ_{lv} = 35.5 mN/m), and hexadecane (γ_{lv} = 27.5 mN/m) on flat silicon wafers sprayed with mixtures of fluoropolymer and FF-silica.

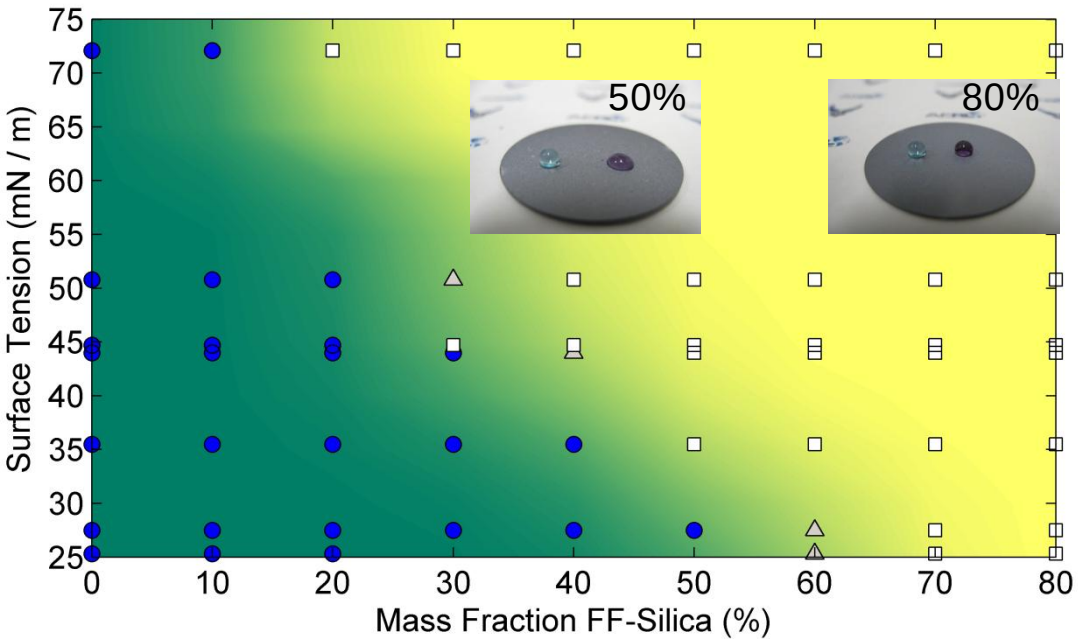

Figure 2. Map depicting the state of liquid contact with FF-silica surfaces as a function of FF-silica loading and surface tension of the contacting liquid; filled circles represent Wenzel states, shaded triangles represent Cassie states with contact angle hysteresis > 20°, unfilled squares represent Cassie states with contact angle hysteresis ≤ 20°. The background color is intended only as an aid for visualization. Inset shows droplets of water (blue) and dodecane (purple) on spray-coated surfaces comprised of 50 wt% FF- silica (left image) and 80 wt% FF-silica (right image) demonstrating the different wetting states as a function of silica loading.

In order to better understand the basis for the simple relationship seen in Fig. 2, the geometry of the sprayed-on surfaces was examined in more detail. Fig. 3 provides both surface view and cross-sectional SEM images of the surfaces as a function of FF-silica loading, with detailed views provided in Fig. 4. The images in Figs. 3 and 4 demonstrate that the FF-silica aggregates (which feature a fluoroalkylated surface to ensure liquid repellence and maintain good dispersion in the spraying solvent) retain sufficient integrity to produce large protrusions from the fluoropolymer layer after deposition and

film formation. It also appears that the low surface tension of the carrier solvent, perhaps in combination with the porosity afforded by the aggregates,[32] allows the fluoropolymer coating to become conformal, particularly as the FF-silica loading level is increased beyond approx. 40%.

In Fig. 4, regions of conformality are indicated by filled arrows, while regions that lack conformality are indicated by unfilled arrows. Since the conformality extends to the base of the protrusions, it appears the typical phenomenon of binder accumulation in the interstitial junctions does not take place. Rather, the protrusions exhibit re-entrant curvature, a key geometric characteristic that enables the Cassie state to be observed with low surface-tension liquids.[1] In addition, the conformality transfers the multi-scale roughness inherent in the aggregates to the coating as a whole. Therefore, the use of silica aggregates in a fluoropolymer binder with a fluorocarbon carrier solvent allows the key characteristic of re-entrant curvature to appear at multiple length scales in sprayed-on FF-silica coatings. In combination with the very low surface energy imparted by the FF-silica and the fluoropolymer, the re-entrant curvature leads to outstanding liquid repellency, including superoleophobicity. To summarize, we believe that as long as the following key conditions are maintained, a wide variety of deposition process parameters will lead to re-entrant textures and superoleophobicity: 1) the use of low surface energy aggregates with multi-scale roughness, 2) the use of low surface energy binders and low surface energy solvents with high vapor pressures at ambient temperature, 3) sufficient coverage of coating to prevent bare spots without depositing so much material that rapid evaporation of solvent is hindered, and 4) sufficiently high aggregate to binder ratio to maintain conformality of the coating.

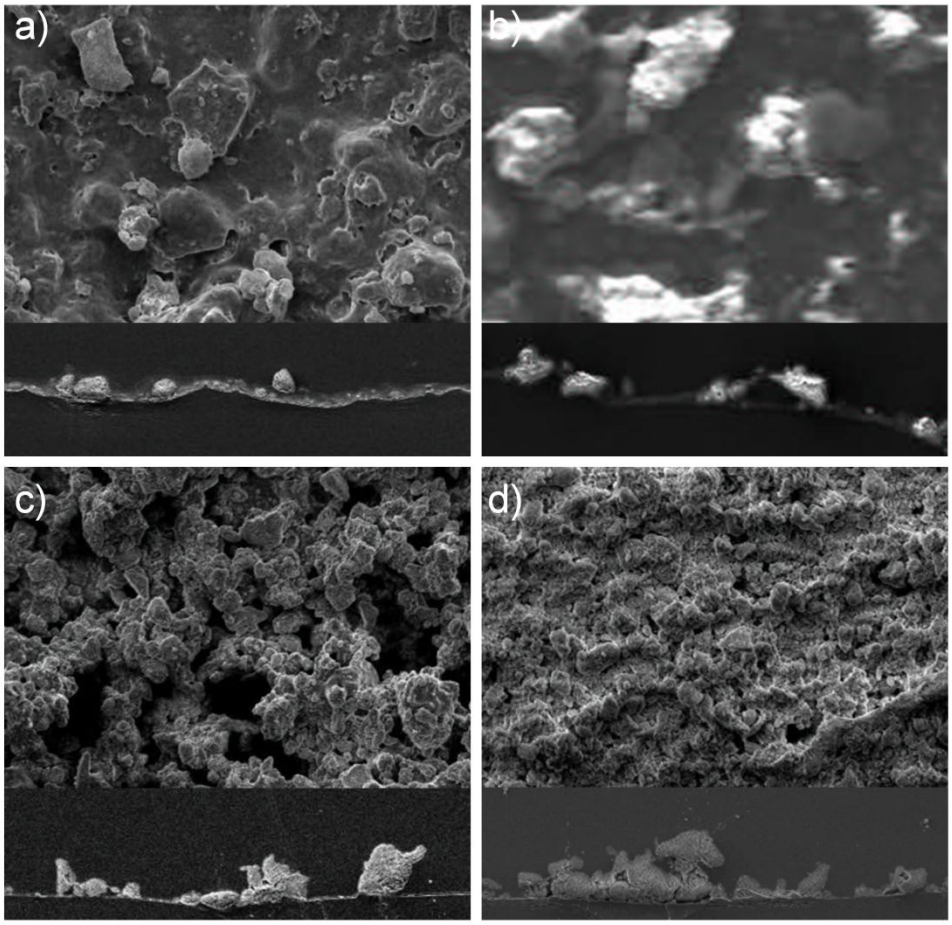

Figure 3. Plan view (top panels) and corresponding cross-sections (lower panels) for FF-silica / fluoroelastomer composites at FF-silica loadings of a) 20 wt% b) 40 wt% c) 60 wt% d) 80 wt%. Note that the images are all at identical magnification, so that the scale bar applies to all images.

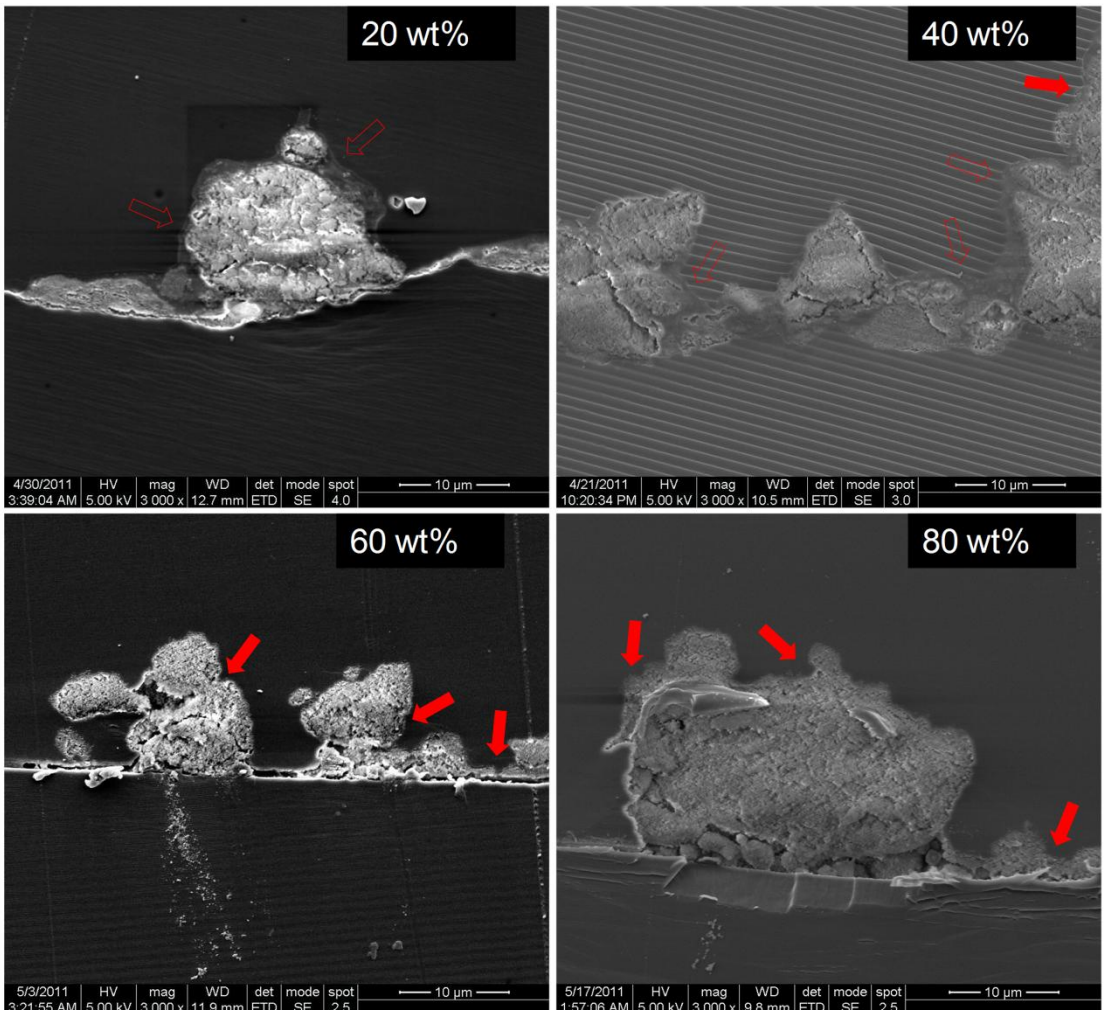

Figure 4. SEM micro-graphs prepared from FF-silica / fluoropolymer coatings mounted in epoxy and cross-sectioned (all at magnification 3000 x). Note the scoring of the epoxy due to the sectioning process, which is helpful in distinguishing it from the fluoropolymer binder that surrounds the silica aggregates. Filled arrows indicate examples of regions where the coating is, if present at all, highly conformal to fine features of the silica surface, whereas unfilled arrows indicate examples where the coating does not conform to the fine features of the silica surface.

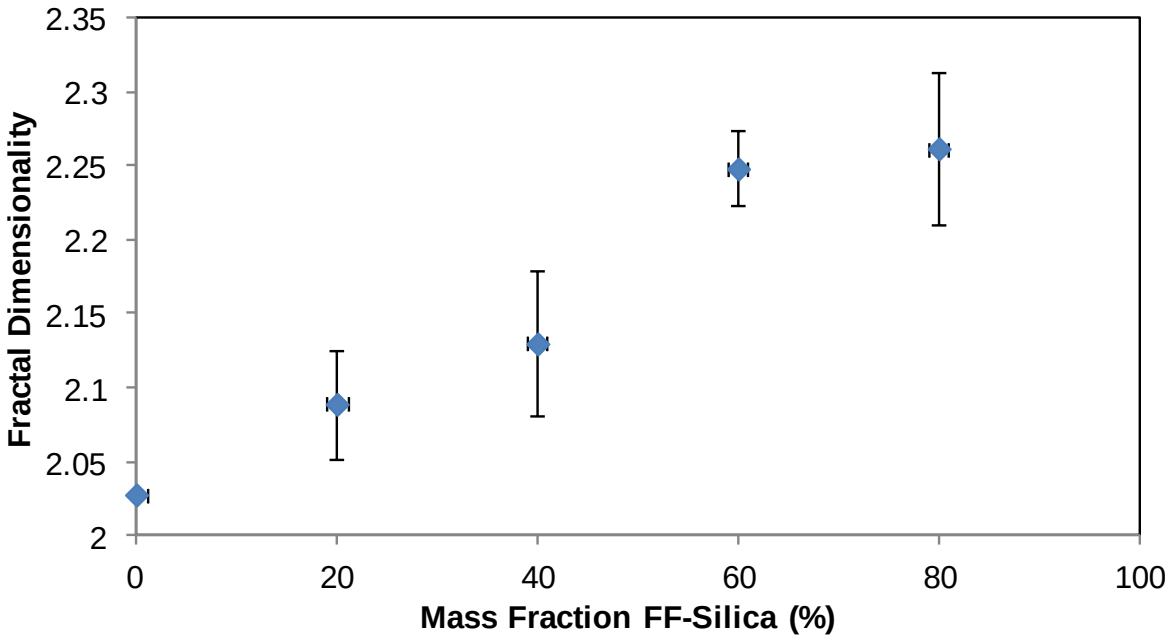

Figure 5. Fractal dimensionality of FF-silica / fluoroelastomer composites as a function of FF-silica loading

3.2 Mathematical analysis of surface texture: Although the preceding qualitative discussion illustrates the key material and process features that lead to superoleophobicity in the spray-coated samples, an explanation of the key features of Fig. 2 requires a mathematical analysis of the surface texture. To aid in this analysis, a quantitative determination of the fractal dimensionality of the surfaces according to the method of Shibuichi[12] was undertaken, with the results shown in Fig. 5. In order to relate the data in Fig. 5 to liquid repellence characteristics, a basic model of the texture of stochastic surfaces was also developed, as described below.

In terms of the systematic design parameter approach for regularly patterned surfaces, a dimensionless parameter D^* can be defined, based on $\phi_{s,total}$, the fraction of the liquid-solid-air composite interface that is occluded by solid, as

$$D^* = 1 / \phi_{s,total} \qquad (1)$$

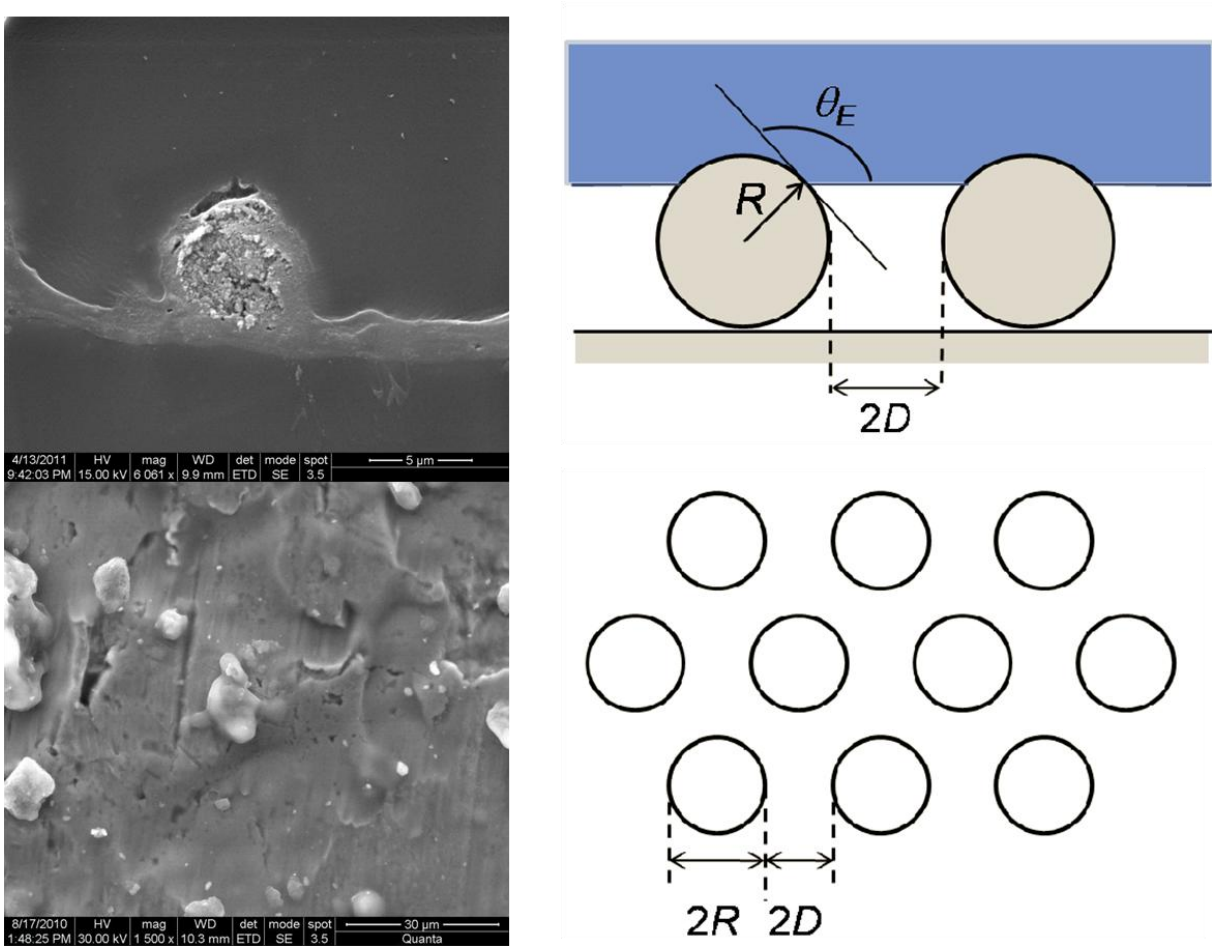

Figure 6. SEM micrographs of spray-coated FF-silica / fluoropolymer composites (left), compared with idealized geometric model used to describe the surface topography of the coatings (right), seen in both cross-section (upper image and illustration) and plan (i.e. "top down") view (lower image and illustration). Note that the illustrations at right originally appeared in Supporting Information (Figure S4) of reference 4.

Based on the value of D^* and the equilibrium contact angle θ_E on an equivalent, homogeneous flat surface, the contact angle on a rough surface θ^* can be predicted via the Cassie-Baxter equation, assuming that θ_E is satisfied locally on micron and sub-micron features,[33] if the geometry of the rough surface is specified. For instance, if a model surface comprised of uniformly distributed, monodisperse spheres (as illustrated in Fig. 6) is specified, then the Cassie-Baxter equation yields:

$$\cos\theta^* = -1+1/D^*[\pi/2\sqrt{3}(1+\cos\theta_E)^2] \quad (2)$$

where D^* can also be defined (for this specific model geometry only) as $[(R+D)/R]^2$ with R being the radius of the sphere and $2D$ the center-to-center distance between spheres

From Eq. (2), an effective model spacing ratio D^*_{model} for the spray-coated surfaces can be calculated with the aid of a plot of $1+\cos\theta^*$ vs $[\pi/(2\sqrt{3})](1+\cos\theta_E)^2$ (using the experimentally determined advancing angles of the FF-silica / fluoroelastomer composites for θ^* and the experimentally determined advancing contact angle for the pure fluoroelastomer for θ_E). In such a plot, the slope as determined via linear regression (with the constant forced to equal zero) is inversely proportional to D^*_{model} , allowing D^*_{model} to be estimated as a function of FF-silica loading, as seen in Fig. 7. Furthermore, based on Eq. (1), the fraction of liquid-solid-air interface occuled by solid ($\phi_{s,model}$) may also be calculated as a function of FF-silica loading, since $\phi_{s,model}$ is directly proportional to the slope found by linear regression. The estimated values of D^*_{model} and $\phi_{s,model}$ as a function of FF-silica loading are shown in Fig. 8.

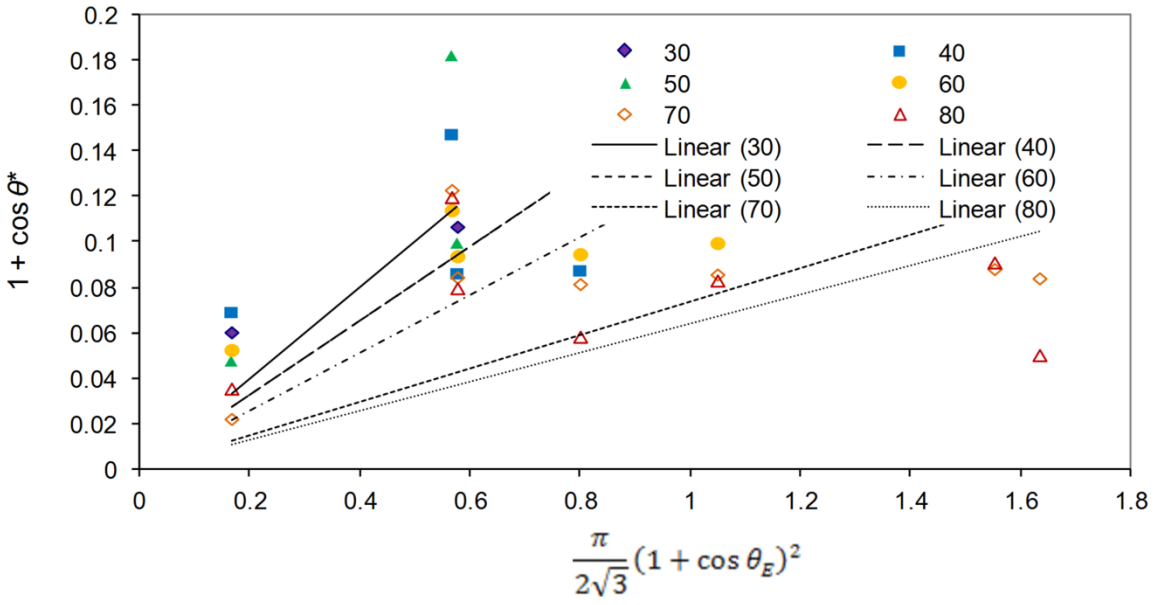

Figure 7 Linear fit used to determine D^*_{model} of the idealized surface having the characteristics of the FF-silica / fluoropolymer coatings (the numbers denote the percentage by weight of FF-silica in the coating).

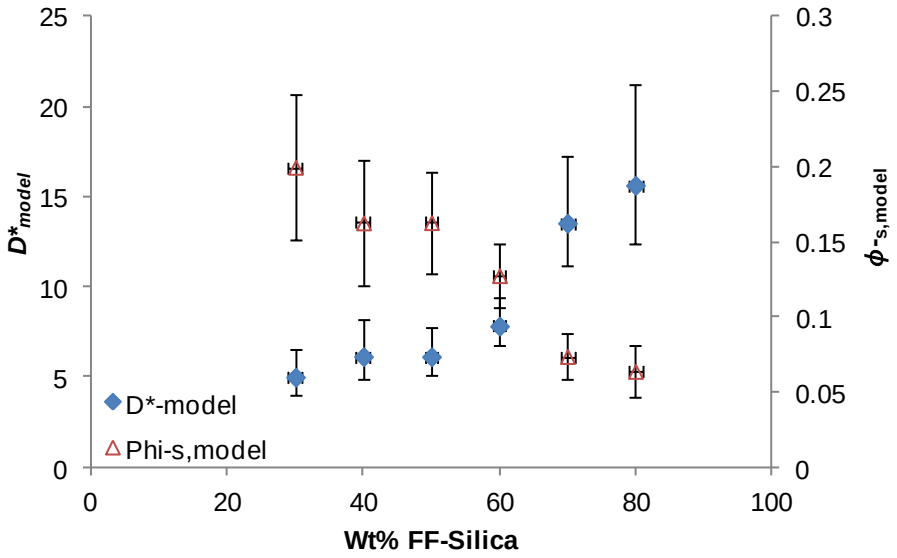

Figure 8. Computed values of D^*_{model} and $\phi_{s,model}$ as a function of FF-silica loading. For clarity in reading the chart, the error bars corresponding to a single standard error in the determination of each parameter, rather than 95% confidence intervals, are shown.

Even though the errors involved are large, Figs. 7 and 8 indicate that as FF-silica content increases, a decreasing fraction of the liquid-solid-air interface is occluded by solid. In other words, more of the interface remains unwet. This result is essentially caused by the fact that liquids with a lower equilibrium contact angle are observed in the Cassie state at higher FF-silica loadings, forcing the slopes of the best fit lines shown in Fig. 7 to decrease with increasing FF-silica loading. Although the specific values shown are model dependent, the trend, being driven by the presence of absence of a Cassie state, will remain the same no matter which geometry is specified. In essence, a Cassie state incorporating larger amounts of air is required to compensate for a lower equilibrium contact angle, hence the presence of Cassie states for liquids with progressively lower equilibrium contact angles at progressively higher loadings indicates that the parameter $\phi_{s,total}$ must decrease with increasing silica loading, indepdent of the specific geometry of the surfaces.

Although the foregoing discussion involves models of discrete particles, it is important to consider the effects of having aggregates with multi-scale roughness, rather than individual monolithic particles, present in the coating. In most calculations of D^* involving discrete particles on a surface, it is assumed that the surface of each particle is fully wetted, while the spaces between particles remain unwet. However, if the surface is comprised of aggregates, and, due to fine-scale roughness, some fraction "u" of the surface of each aggregate remains unwet, then D^* can be expressed in a modified form given by

$$D^* = 1 / [\ (1–u)\ \phi_{s0}\ ] = [\ 1 / (1\text{-}u)\ ]\ D_0^* \qquad (3)$$

In Eq. (3), the quantities with subscript *0* refer to equivalent values for a surface comprised of monolithic particles with an arrangement identical to that of the aggregates. Because $0 \leq u \leq 1$, D^* will be as high or higher for a surface conformal to aggregates as compared to an identical surface that conforms to monolithic particles. The value of u will depend on specific details of the surface topography at the line of contact,[34] not simply the porosity of the aggregate, hence reliable *a priori* methods for calculating u are not readily available. For uniformly distributed, monolithic, and monodisperse spherical particles, however, the parameter D_0^* can be thought of as the square of an effective spacing ratio, that is the distance between particles divided by the particle diameter (see Supporting Information, Section S2). Although these input parameters for D_0^* will not be well-defined for a surface comprised of random, polydisperse (but monolithic) aggregates, the average distance between aggregates will decrease as approximately the square root of the aggregate concentration (for monolayer-like arrangements of aggregates as seen in Fig. 3), while the aggregate size distribution remains constant. The result is that D_0^* should decrease with increased aggregate loading, first rapidly, and then gradually.

By examining Fig. 1 more closely, it can be seen that, once the Cassie state is attained, further increases in silica loading result in modest increases in apparent contact angles. In a composite interface, the higher apparent contact angle results from a decrease in $\phi_{s,total}$, or equivalently, an increase in D^* [1-3]. Thus, the purely empirical data indicate that D^* increases with increased FF-silica loading,

just as the results based on analysis of model surfaces do, but both are contrary to the expected behavior of D_0*. Therefore, based on Eq. (3), *u* must increase with increased FF-silica content in order to cause the observed increase in *D**. In the specific case of a hierarchical surface with well-defined features replicated at multiple length scales, it has been proven mathematically that *u* will increase as features are replicated at smaller and smaller length scales.[35] The fractal dimensionality of the textured surface also represents another useful single geometric parameter that indicates the level of fine-scale roughness (see Supporting Information Section S4 for an explanation). Therefore, the increasing fractal dimensionality of the surfaces with increased FF-silica content seen in Fig. 5 implies that *u* also increases with increasing FF-silica content, and thus explains the observed contact angle behavior. An increasing value of *u* should also stabilize the Cassie state for lower surface tension liquids, and result in the behavior reflected in Fig. 2, or, equivalently, stabilize the Cassie state for liquids with lower values of θ_E, resulting in the observed behavior of D^*_{model} and $\phi_{s,model}$ seen in Figs. 7 and 8.

3.3 Implications for Coating Design and Performance. In addition to the geometric analysis, a careful examination of the cross-sectional images seen in Fig. 4 revealed a qualitative change in the nature of the topography as the FF-silica content was increased. (Note that these changes were seen over the course of examining almost 100 separate images, with Fig. 4 providing representative examples). At loading levels below 40 wt% silica, there appears to be an "excess" of fluoropolymer binder, which fills in small gaps between aggregates and sub-aggregates and provides a relatively thick coating of the substrate that partly submerges the smaller aggregates. The result is a surface that is conformal only above a length scale of a micron or so. Above 40 wt% FF-silica, however, there appears to be almost no "excess" binder. In this case, the highly conformal coating preserves the roughness of the aggregates down to sub-micron scales. Although the most prominent change occurs at approx. 40 wt% FF-silica, where the aggregates also begin to clump together, the coating can be seen to conform to progressively smaller-sized features as the FF-silica loading increases. The gradual spread of conformality to smaller length scales due to an increasingly severe shortage of binder thus appears to be the mechanism responsible for the observed changes in fractal dimensionality, contact angle, and

minimum surface tension of contacting fluids exhibiting the Cassie state, as a function of FF-silica loading.

The above discussion illustrates that innovative methods can be utilized to systematically alter the topography of randomly textured surfaces to obtain desired liquid repellence characteristics. Even in the context of spatially-variable robustness, which appears to be characteristic of such surfaces (see the discussion of immersion depth and evaporating droplets in Supporting Information Section S1), it appears that the contact and sliding angles can be altered in systematic fashion by controlling parameters, such as the fractal dimensionality or the distribution of roughness, across multiple length scales. For sprayed on surfaces consisting of rigid aggregates with a polymeric binder, the aggregate to binder ratio influences these parameters due to a mechanism by which local accumulations of binder mask the fine-scale roughness of the aggregates. The aforementioned mechanism is expected to apply to all types of coatings containing rigid aggregates dispersed in a soft binder, provided that significant migration of binder into large interstices is avoided. Because the mechanism involves a simple excess or shortage of binder, it is expected to be insensitive to the details of the coating process itself, as long as the aggregates are deposited in a monolayer-like fashion.

The above discussion also has significant implications for coating performance. Generally speaking, the durability and adhesion characteristics of aggregate-reinforced polymer coatings are best when there is not a shortage of binder. In order to attain superoleophobicity, however, a shortage of binder is helpful, because it results in greater conformality at small length scales, which in turn increases the non-wetting fraction of the aggregate surface, leading to higher contact angles and promoting formation of the Cassie state. In observing the behavior of the spray-coated samples, we noted that the cohesion of the coatings dropped substantially above an FF-silica loading of about 40 wt%, the point at which a shortage of binder appears to emerge. Although samples with less than about 40 wt% FF-silica could easily be removed from the substrate due to the low adhesion of the fluoroelastomer to silicon wafers, the coatings themselves tended to resist abrasion. On the other hand, when greater than 40 wt% FF-silica was present, the coatings tended to scratch easily and become dislodged from the substrate in

small pieces. Although there does appear to be a trade-off between liquid repellence and mechanical performance in the samples studied, there are many methods available to improve the mechanical performance of sprayed-on polymer coatings (such as cross-linking and adding specific coupling agents) that should have minimal effects on liquid repellence. The creation of superoleophobic coatings made by very simple deposition processes that also exhibit optimized adhesion and cohesion characteristics thus remains an important area for future development efforts.

4. Conclusions

Coatings comprising a sprayed-on mixture of fluoroalkyl-functional precipitated silica and a fluoropolymer binder have proven to be an especially useful class of liquid repellent coating. The combination of low surface energy materials, aggregate porosity, and rapid deposition via spray coating appears to prevent the build-up of binder in interstitial regions, preserving re-entrant curvature across multiple length scales and thereby enabling a wide range of liquid repellency, including superoleophobicity, to be attained via a simple and scalable process. In addition, rather than accumulating in the interstices, the binder becomes widely distributed across the surface of the aggregates, enabling a mechanism in which a simple shortage or excess of binder controls the extent of coating roughness at very small length scales, thereby controlling the extent of liquid repellence through a change in the non-wetting fraction of the aggregates. The exploitation of these advantages is expected to lead to significant progress towards large-scale commercialization of superoleophobic surfaces.

Supporting Information Available

Properties of fluoroalkylsilane-functionalized silica (FF-silica, Table S1), complete contact angle data with uncertainties (Table S2), original SEM micrographs of surfaces (Figures S1 and S2), robustness properties of FF-silica composites with accompanying video (Section S1), derivation of the dependence of average distance between particles on particle loading (Section S2), and derivation of the linkage

between fractal dimensionality and extent of fine-scale roughness (Section S3). This material is available free of charge via the Internet at http://pubs.acs.org.

Acknowledgements

Support for this work from the Air Force Office of Scientific Research, the Air Force Research Laboratory, Propulsion Directorate, and the National Research Council is gratefully appreciated. The authors thank Mr. Brian Moore of AFRL for helping prepare the video files included in Supporting Information.

References

1. Tuteja, A.; Choi, W.; Ma, M. L.; Mabry, J. M.; Mazzella, S. A.; Rutledge, G. C.; McKinley, G. H.; Cohen, R. E., Designing Superoleophobic Surfaces. *Science* **2007**, *318*, 1618-1622.

2. Tuteja, A.; Choi, W.; Mabry, J. M.; McKinley, G. H.; Cohen, R. E., Robust omniphobic surfaces. *Proc. Nat. Acad. Sci.U. S. A.* **2008**, *105*, 18200-18205.

3. Tuteja, A.; Choi, W.; McKinley, G. H.; Cohen, R. E.; Rubner, M. F., Design Parameters for Superhydrophobicity and Superoleophobicity. *MRS Bull.* **2008**, *33*, 757.

4. Chhatre, S. S.; Choi, W.; Tuteja, A.; Park, K.-C. K.; Mabry, J. M.; McKinley, G. H.; Cohen, R. E., Scale Dependence of Omniphobic Mesh Surfaces. *Langmuir* **2010**, *26*, 4027-4035.

5. Bhushan, B.; Jung, Y. C., Natural and biomimetic artificial surfaces for superhydrophobicity, self-cleaning, low adhesion, and drag reduction. *Prog. Mater Sci.* **2011,** 56, 1-108.

6. Zhao, H.; Law, K.-Y.; Sambhy, V., Fabrication, Surface Properties, and Origin of Superoleophobicity for a Model Textured Surface. *Langmuir* **2011,** 27, 5927-5935.

7. Chhatre, S. S.; Tuteja, A.; Choi, W.; Revaux, A.; Smith, D.; Mabry, J. M.; McKinley, G. H.; Cohen, R. E., Thermal Annealing Treatment to Achieve Switchable and Reversible Oleophobicity on Fabrics. *Langmuir* **2009,** 25 (23), 13625-13632.

8. Choi, B. W.; Tuteja, A.; Chhatre, S.; Mabry, J. M.; Cohen, R.; McKinley, G. H., Fabrics with Tunable Oleophobicity. *Adv. Mater.* **2009,** 21, 2190-2195.

9. Nosonovsky, M.; Bhushan, B., Superhydrophobic surfaces and emerging applications: Non-adhesion, energy, green engineering. *Current Opinion in Colloid & Interface Science* **2009,** 14, 270-280.

10. Howarter, J. A.; Genson, K. L.; Youngblood, J. P., Wetting Behavior of Oleophobic Polymer Coatings Synthesized from Fluorosurfactant-Macromers. *ACS Applied Materials & Interfaces* **2011,** 3, 2022-2030.

11. Tsujii, K.; Yamamoto, T.; Onda, T.; Shibuichi, S., Super oil-repellent surfaces. *Angew. Chem.-Int. Edit. Engl*. **1997,** 36, 1011-1012.

12. Shibuichi, S.; Yamamoto, T.; Onda, T.; Tsujii, K., Super water- and oil-repellent surfaces resulting from fractal structure. *J. Colloid Interface Sci.* **1998,** 208, 287-294.

13. Sheen, Y.-C.; Huang, Y.-C.; Liao, C.-S.; Chou, H.-Y.; Chang, F.-C., New Approach to Fabricate an Extremely Super-amphiphobic Surface Based on Fluorinated Silica Nanoparticles. *J. Polym. Sci. Part B: Polym. Phys.* **2008,** 46, 1984-1990.

14. Steele, A.; Bayer, I.; Loth, E., Inherently Superoleophobic Nanocomposite Coatings by Spray Atomization. *Nano Lett.* **2009,** 1, 501-505.

15. Hsieh, C.-T.; Wu, F.-L.; Chen, W.-Y., Superhydrophobicity and superoleophobicity from hierarchical silica sphere stacking layers. *Mater. Chem. Phys.* **2010,** 121, 14-21.

16. Srinivasan, S.; Chhatre, S. S.; Mabry, J. M.; Cohen, R. E.; McKinley, G. H., Solution spraying of poly(methyl methacrylate) blends to fabricate microtextured, superoleophobic surfaces. *Polymer* **2011,** 52, 3209-3218.

17. Yang, J.; Zhang, Z.; Men, X.; Xu, X.; Zhu, X., A simple approach to fabricate superoleophobic coatings. *New J. Chem.* **2011,** 35, 576-580.

18. Yang, J.; Zhang, Z. Z.; Xu, X. H.; Men, X. H.; Zhu, X. T.; Zhou, X. Y., Superoleophobic textured aluminum surfaces. *New J. Chem.* **2011,** 35, 2422-2426.

19. Deng, X.; Mammen, L.; Butt, H. J.; Vollmer, D., Candle Soot as a Template for a Transparent Robust Superamphiphobic Coating. *Science* **2012,** 33, 67-70.

20. Das, A.; Schutzius, T. M.; Bayer, I. S.; Megaridis, C. M., Superoleophobic and conductive carbon nanofiber/fluoropolymer composite films. *Carbon* **2012,** 50, 1346-1354.

21. Bellanger, H.; Darmanin, T.; Guittard, F., Surface Structuration (Micro and/or Nano) Governed by the Fluorinated Tail Lengths toward Superoleophobic Surfaces. *Langmuir* **2012,** 28, 186-192.

22. Artus, G. R. J.; Zimmermann, J.; Reifler, F. A.; Brewer, S. A.; Seeger, S., A superoleophobic textile repellent towards impacting drops of alkanes. *Appl. Surf. Sci.* **2012,** 258, 3835-3840.

23. Goto, Y.; Takashima, H.; Takishita, K.; Sawada, H., Creation of coating surfaces possessing superhydrophobic and superoleophobic characteristics with fluoroalkyl end-capped vinyltrimethoxysilane oligomeric nanocomposites having biphenylene segments. *J. Colloid Interface Sci.* **2011,** 362, 375-381.

24. Zhu, X. T.; Zhang, Z. Z.; Xu, X. H.; Men, X. H.; Yang, J.; Zhou, X. Y.; Xue, Q. J., Facile fabrication of a superamphiphobic surface on the copper substrate. *J. Colloid Interface Sci*. **2012,** 367, 443-449.

25. Yang, J.; Zhang, Z. Z.; Xu, X. H.; Zhu, X. T.; Men, X. H.; Zhou, X. Y., Superhydrophilic-superoleophobic coatings. *J. Mater. Chem.* **2012,** 22, 2834-2837.

26. Yao, X.; Gao, J.; Song, Y. L.; Jiang, L., Superoleophobic Surfaces with Controllable Oil Adhesion and Their Application in Oil Transportation. *Adv. Funct. Mater.* **2011,** 21, 4270-4276.

27. Yuan, Z. Q.; Xiao, J. Y.; Wang, C. Q.; Zeng, J. C.; Xing, S. L.; Liu, J., Preparation of a superamphiphobic surface on a common cast iron substrate. *J. Coat. Technol. Res.* **2011,** 8, 773-777.

28. Campos, R.; Guenthner, A. J.; Haddad, T. S.; Mabry, J. M., Fluoroalkyl-Functionalized Silica Particles: Synthesis, Characterization, and Wetting Characteristics. *Langmuir* **2011,** 27, 10206-10215.

29. See, for example, U. S. Patent 6,025,025 and references therein.

30. Hozumi, A.; McCarthy, T. J., Ultralyophobic Oxidized Aluminum Surfaces Exhibiting Negligible Contact Angle Hysteresis. *Langmuir* **2010,** 26, 2567-2573.

31. Basu, B. B. J.; Paranthaman, A. K., A simple method for the preparation of superhydrophobic PVDF-HMFS hybrid composite coatings. *Appl. Surf. Sci.* **2009,** 255, 4479-4483.

32. The BET surface area of the treated aggregate, as reported in Ref. 25, was 92 m^2/g.

33. Marmur, A., Wetting on hydrophobic rough surfaces: To be heterogeneous or not to be? *Langmuir* **2003,** *19*, 8343-8348.

34. Choi, W.; Tuteja, A.; Mabry, J. M.; Cohen, R. E.; McKinley, G. H., A modified Cassie–Baxter relationship to explain contact angle hysteresis and anisotropy on non-wetting textured surfaces. *J. Colloid Interface Sci.* **2009,** 339, 208-216.

35. Herminghaus, S., Roughness-induced non-wetting, *Europhys. Lett.* **2000**, 52(2), 165-170.

Table of Contents Graphic – for table of contents use only

"Superoleophobic Surfaces through Control of Sprayed-on Stochastic Topography"

Raymond Campos, Andrew J. Guenthner, Adam J. Meuler, Anish Tuteja, Robert E. Cohen, Gareth H. McKinley, Timothy S. Haddad, and Joseph M. Mabry

AUTHOR EMAIL ADDRESS andrew.guenthner@edwards.af.mil